Bioorganic & Medicinal Chemistry 18 (2010) 4957–4964

Contents lists available at ScienceDirect

Bioorganic & Medicinal Chemistry

journal homepage: www.elsevier.com/locate/bmc

Identification and evaluation of apoptotic compounds from *Garcinia paucinervis*

Xue-Mei Gao [a,d,†], Ting Yu [b,†], Fanny Shuk Fan Lai [a], Yan Zhou [a], Xin Liu [a], Chun-Feng Qiao [a], Jing-Zheng Song [a], Shi-Lin Chen [c], Kathy Qian Luo [b,*], Hong-Xi Xu [a,*]

[a] Chinese Medicine Laboratory, Hong Kong Jockey Club Institute of Chinese Medicine, Shatin, N.T., Hong Kong, People's Republic of China
[b] Division of Bioengineering, School of Chemical and Biomedical Engineering, Nanyang Technological University, 70 Nanyang Drive, Singapore 637457, Singapore
[c] Institute of Medicinal Plant Development, Chinese Academy of Medical Sciences, Beijing 100094, People's Republic of China
[d] School of Chemistry and Biotechnology, Yunnan Nationalities University, Kunming 650031, China

ARTICLE INFO

Article history:
Received 9 March 2010
Revised 3 June 2010
Accepted 4 June 2010
Available online 10 June 2010

Keywords:
Apoptosis
HeLa cell
Garcinia paucinervis
Caspase-3

ABSTRACT

Four new compounds, paucinervins A–D (**1**–**4**), and 15 known ones were isolated from the leaves of *Garcinia paucinervis*. The structures of the new compounds were elucidated by spectroscopic evidences. All of the 19 compounds were evaluated for their apoptosis-inducing effects using HeLa-C3 cells which have been genetically engineered to possess a fluorescent biosensor capable of detecting caspase-3 activation. Eight of them were found to activate caspase-3 in HeLa-C3 cells within 72 h at the concentration of 25 μM. Moreover, the values of IC_{50} were measured for all four new compounds on HeLa cells using the MTT assay. Among them, compound **2** (paucinervin B) had the lowest IC_{50} value of 9.5 μM, while the other three new compounds had much higher IC_{50} values of 29.5, 52.5, and 95.6 μM, respectively. This result shows that paucinervin B has the strongest inhibitory effect against HeLa cell growth among these four newly identified paucinervins and it may have the potential to be developed into a new anticancer candidate.

1. Introduction

Apoptosis is a programmed cell death that leads to the removal of unwanted and abnormal cells.[1] Preferential and efficient inductions of apoptosis in tumor cells are regarded as one of the most effective anticancer therapies. Activation of caspase-3 is the most critical event signifying the occurrence of apoptosis which forms the basis for measuring the apoptotic extent.[2] Compounds isolated from natural sources leading to caspase-3 activation may be potential reservoirs of anticancer drugs.

The *Garcinia* genus is well known to be a rich source of bioactive isoprenylated xanthones and benzophenones.[3–9] Previously, we reported to identify a series of benzophenones and xanthones isolated from the *Garcinia* genus as apoptosis inducers of HeLa cells.[3–6] *Garcinia paucinervis* is a valuable species distributing in Yunnan and Guangxi provinces of China.[10] As a part of the phytochemical and pharmacological investigations of *Garcinia* plants in China, a bioassay-guided screening of the bioactive compounds in leaves of *G. paucinervis* was conducted resulting in the isolation of 19 compounds inclusive of four new ones. The present report describes the isolation and structure elucidation of these compounds as well as the evaluation of their anticancer potentials.

2. Results and discussion

2.1. Bioassay-guided isolation of bioactive compounds and structural elucidation of new compounds

An acetone extract prepared from the leaves of *G. paucinervis* was partitioned between EtOAc and H_2O. The EtOAc layer was subjected repeatedly to column chromatography over silica gel, Sephadex LH-20, and RP-18 and to HPLC to afford four new compounds, paucinervins A–D (**1**–**4**), together with 15 known ones, namely guttiferone E[11] (**5**), guttiferone I[12] (**6**), 30-*epi*-cambogin[13] (**7**), (+)-guttiferone K[14] (**8**), cambogin[14] (**9**), garcicowin C[15] (**10**), formoxanthone A[16] (**11**), parvifolixanthone A[17] (**12**), 1,3,7-trihydroxy-2-prenylxanthone[18] (**13**), jacareubin[19] (**14**), nigrolineaxanthone E[20] (**15**), cembrene A[21] (**16**), parvifoliol F[17] (**17**), 2-cyclohexene-γ,η,2,6,6-pentamethyl-1-nonanol[22] (**18**), and vitamin E quinone[23] (**19**).

Compound **1** was obtained as yellow gum. Its molecular formula was established as $C_{24}H_{26}O_7$ by HRESIMS at *m*/*z* 427.1694 $[M+H]^+$, suggesting the presence of 12 degrees of unsaturations. The ^1H and ^{13}C NMR data of **1** (Table 1) showed the presence of 5 methyls, 2 methylenes, 4 olefinic methines, 1 carbonyl carbon and 12 olefinic quaternary carbons. The IR spectrum showed absorption bands for hydroxyl groups (3411 cm^{-1}) and a lactone carbonyl group chelated to an ortho-hydroxyl group (1624 cm^{-1}). The presence of the latter functionality was confirmed by resonances at δ_C 168.5 (C-9) and δ_H 11.32 (OH-1). The NMR spectra showed two sets of signals corresponding to prenyl groups. The

* Corresponding authors. Tel.: +65 6790 4257; fax: +65 6791 1761 (K.Q.L.); tel.: +852 3406 2873; fax: +852 3551 7333 (H.-X.X.).
E-mail addresses: kluo@ntu.edu.sg (K.Q. Luo), xuhongxi@hkjcicm.org (H.-X. Xu).
† Xue-Mei Gao and Ting Yu contributed equally to this paper.

0968-0896/$ - see front matter © 2010 Elsevier Ltd. All rights reserved.
doi:10.1016/j.bmc.2010.06.014

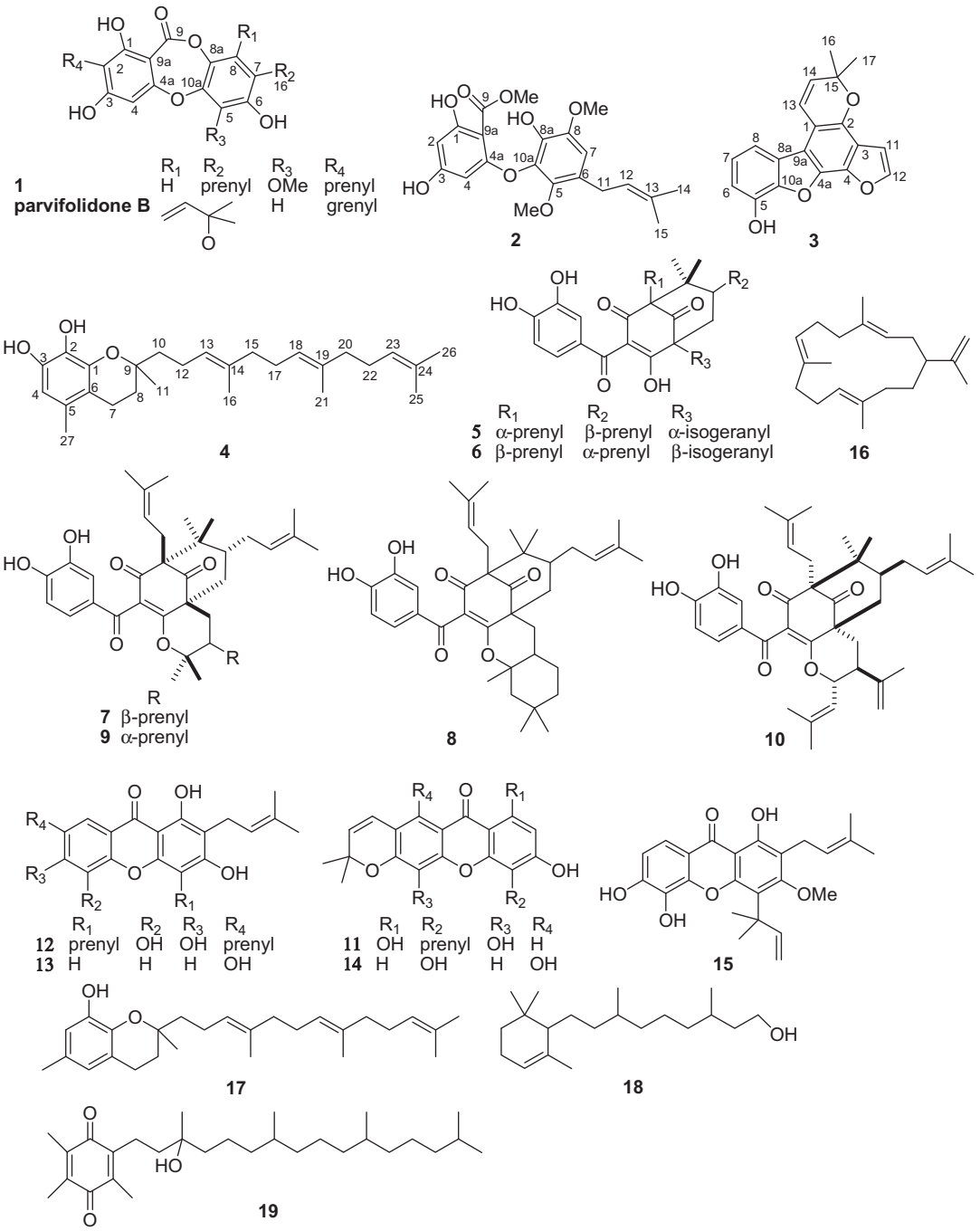

foregoing data indicated that **1** was a depsidone derivative that contained two isoprene units.

Analyzing the 2D NMR spectra using HMQC and HMBC techniques enabled the assignment of ^{1}H and ^{13}C NMR signals. By comparing the NMR data of **1** with those of the known compound, parvifolidone B,[18] the possible structure of **1** was established suggesting the same core structure for both compounds. In the HMBC spectrum, the chelated proton signal at δ_H 11.32 corresponding to OH-1 showed a strong cross-peak with the carbon at δ_C 98.7 (C-9a), which represents the linkage of aromatic carbon to the carbonyl group (Fig. 1). The OH-1 proton also exhibited HMBC connectivity to δ_C 162.8 (oxygenated aromatic carbon C-1) and δ_C 111.3 (substituted aromatic carbon C-2) (Fig. 1). The HMBC cross-peaks of C-2/(H-11, -12) confirmed that the C-2 group was substituted by a prenyl group. The aromatic proton at δ_H 6.35 (C-4) showed HMBC connectivity to four aromatic carbons at δ_C 98.7 (C-9a), 159.4 (C-4a), 162.0 (C-3), and 111.3 (C-2). The second prenyl group was determined to be presented at C-7 based on the HMBC connectivity of the carbon at δ_C 124.8 (C-7) to H-16 and H-17 (Fig. 1). A methoxy group resonating at δ_H 4.08 in the ^{1}H NMR spectrum of **1** was located at C-5 according to its HMBC correlation with C-5 (Fig. 1). The quaternary carbon signals of δ_C 144.8 (C-6), 162.0 (C-3) and its molecular formula $C_{24}H_{26}O_7$ indicated the presence of two hydroxyl groups at C-3 and C-6, respectively. Thus, compound **1**, identified as a new compound, was named paucinervin A.

Paucinervin B (**2**) was obtained as brown gum. The molecular formula of **2** was determined to be $C_{21}H_{24}O_8$ by HRESIMS at m/z 405.1540 $[M+H]^+$. It exhibited UV and IR absorption bands similar to those of **1**. Comparison of the NMR data between **2** and **1** indicated that they are different in the substitutes on the aromatic

Table 1
^{1}H and ^{13}C NMR Data for paucinervins A–C (**1**–**3**)[a]

No.	**1**[b]		**2**[c]		**3**[c]	
	δ_C	δ_H	δ_C	δ_H	δ_C	δ_H
1	162.8 s		164.7 s		111.1 s	
2	111.3 s		95.0 d	5.56 (d, 2.3)	143.5 s	
3	162.0 s		162.6 s		119.3 s	
4	100.5 d	6.35 (s)	97.6 d	5.96 (d, 2.3)	141.1 s	
4a	159.4 s		165.7 s		136.5 s	
5	137.8 s		145.6 s		159.7 s	
10a	140.6 s		133.7 s		153.5 s	
6	144.8 s		124.0 s		128.4 d	7.22 (t, 8.1)
7	124.8 s		112.4 d	6.50 (s)	103.9 d	7.07 (d, 8.1)
8	115.6 d	6.79 (s)	147.6 s		110.0 d	6.75 (d, 8.1)
8a	137.6 s		134.8 s		114.3 s	
9	168.5 s		172.6 s			
9a	98.7 s		97.8 s		119.4 s	
11	22.0 t	3.38 (d, 7.2)	29.2 t	3.26–3.29 (m)	105.7 d	6.92 (d, 2.1)
12	120.9 d	5.19–5.26 (m)	124.0 d	5.22–5.27 (m)	145.9 d	7.70 (d, 2.1)
13	136.0 s		133.4 s		124.3 d	8.10 (d, 10.1)
14	17.9 q	1.80 (s)	25.9 q	1.73 (s)	128.0 d	5.62 (d, 10.1)
15	25.7 q	1.74 (s)	17.8 q	1.74 (s)	76.7 s	
16	27.6 t	3.27 (d, 7.4)			27.7 q	1.46 (s)
17	120.8 d	5.19–5.26 (m)			27.7 q	1.46 (s)
18	134.1 s					
19	17.7 q	1.68 (s)				
20	25.7 q	1.74 (s)				
OMe	62.6 q	4.08 (s)	61.5 q	3.77 (s)		
OMe			61.4 q	3.74 (s)		
COOMe			52.4 q	3.89 (s)		
OH-1		11.32 (s)				

[a] Data were recorded with a Bruker DRX-400 MHz spectrometer, chemical shifts (δ) were expressed in ppm, J in Hz; assignments were confirmed by ^{1}H–^{1}H COSY, HMQC, and HMBC.
[b] Data were recorded in $CHCl_3$.
[c] Data were recorded in CD_3OD.

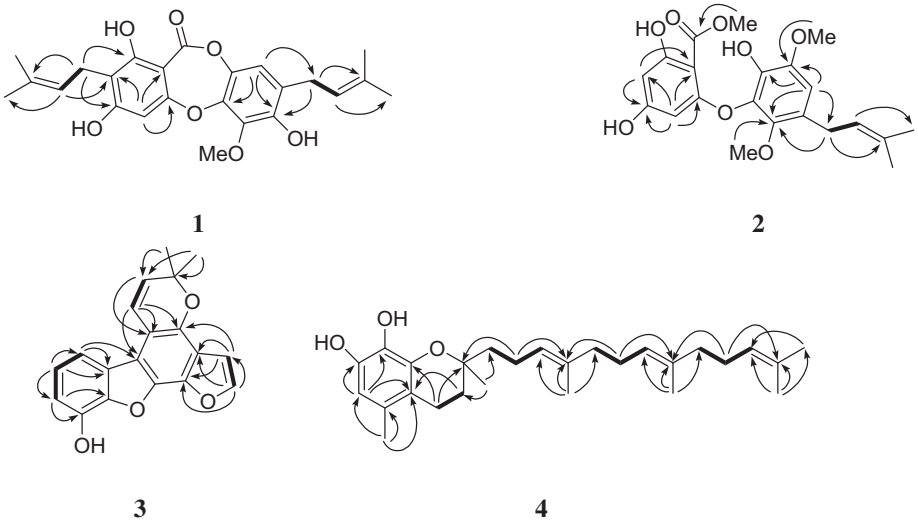

Figure 1. Selected HMBC (→) and ^{1}H–^{1}H COSY (—) correlations of **1**–**4**.

rings. The presence of one prenyl group was deducted from its NMR spectra, which was located at C-6 of the aromatic ring in **2** based on the HMBC correlations of H_2-11 to C-5, C-6 and C-7 (Fig. 1). Two methoxy groups were located at C-5 (δ_C 145.6) and C-8 (δ_C 147.6) on the basis of their HMBC correlations with these two carbon signals, respectively (Fig. 1). Resonances for the singlet aromatic proton and one of the prenyl groups in **1** were replaced by signals of two meta-aromatic protons [δ_H 5.56 (d, J = 2.3 Hz) and 5.96 (d, J = 2.3 Hz)] in **2**. The higher field aromatic proton was attributed to H-2 according to its HMBC correlations with C-1 (δ_C 164.7), C-4 (δ_C 97.6), and C-9a (δ_C 97.8) (Fig. 1). The other meta-aromatic proton was then located at C-4. The third methoxy group (δ_H 3.89, δ_C 52.4) was located at C-9 according to HMBC correlation (Fig. 1). The ^{13}C NMR signal of C-9 (δ_C 172.6) in **2**, appearing in lower field than that of C-9 in **1**, confirmed that the ester group between C-8a and C-9a was broken in **2**. The quaternary carbon signal of δ_C 164.7 (C-1), 162.6 (C-3), 134.8 (C-8a) and the molecular formula $C_{21}H_{24}O_8$ indicated the presence of three hydroxyl groups at C-1, C-3, and C-8a, respectively. Therefore, the structure of **2** was established as shown.

Paucinervin C (**3**) was obtained as yellow gum. HRESIMS analysis of **3** at m/z 305.0509 $[M-H]^-$ demonstrated that it has the

Table 2
^{1}H and ^{13}C NMR data for paucinervin D (**4**) in CD_3OD[a]

No.	4		No.	4	
	δ_C	δ_H		δ_C	δ_H
1	148.2 s		15	40.7 t	1.92–1.97 (overlap)
2	124.4 s		16	15.9 q	1.54 (s)
3	157.4 s		17	27.5 t	2.04–2.09 (overlap)
4	116.3 d	6.43 (s)	18	125.5 d	5.06 (t, 7.2)
5	146.3 s		19	135.8 s	
6	121.3 s		20	40.8 t	1.92–1.97 (overlap)
7	21.8 t	2.58 (t, 6.9)	21	11.2 q	2.02 (s)
8	32.9 t	1.74–1.80 (m)	22	27.8 t	2.04–2.09 (overlap)
9	75.2 s		23	125.4 d	5.06 (t, 7.2)
10	40.2 t	1.48–1.52 (m)	24	132.0 s	
11	24.2 q	1.22 (s)	25	17.8 q	1.56 (s)
12	23.2 t	2.09–2.13 (m)	26	25.9 q	1.64 (s)
13	125.9 d	5.11 (t, 7.2)	27	16.1 q	2.04 (s)
14	135.9 s				

[a] Data were recorded with a Bruker DRX-400 MHz spectrometer, chemical shifts (δ) were expressed in ppm, J in Hz; assignments were confirmed by ^{1}H–^{1}H COSY, HMQC, and HMBC.

molecular formula $C_{19}H_{14}O_4$. The absence of ester carbonyl group in the ^{1}H and ^{13}C NMR data of **3** suggested that it has different carbon skeleton from **1** and **2**. In the ^{13}C NMR spectrum (Table 1), 12 signals from the aromatic region, a signal from the *gem*-dimethylchromene moiety and another signal from the furan ring were observed. The pattern of the aromatic carbon signals showed similarity to those of the xanthone nucleus except for the absence of a carbonyl signal in this compound. These data suggested that compound **3** was a dibenzofuran substituted with a *gem*-dimethylchromene moiety and a furan ring.

The presence of a *gem*-dimethylchromene moiety in **3** was evidenced by a sharp 6H singlet at δ_H 1.46 and an AB spin system at δ_H 5.62 (J = 10.1 Hz, H-14) and δ_H 8.10 (J = 10.1 Hz, H-13). Two single-proton doublet at δ_H 6.92 and δ_H 7.70 (J = 2.1 Hz) could be assigned to the H-11 and H-12 protons, respectively, of the typical furan ring. Furthermore, the signals at δ_H 6.75 (C-8), 7.07 (C-7), and 7.22 (C-6) suggested the presence of three ortho-aromatic protons in the left aromatic ring. Their positions were determined by the HMBC correlations of H-6 with C-5, C-10a, C-7, C-8, of H-7 with C-5, C-6, C-8, C-8a, and of H-8 with C-6, C-7, C-8a, C-10a (Fig. 1). The quaternary carbon signal of δ_C 159.7 (C-5) and the molecular formula $C_{19}H_{14}O_4$ indicated the presence of a hydroxyl group at C-5. The HMBC correlations of H-11 and H-12 with C-3 and C-4, respectively, indicated that the furan ring was fused in an angular form on the right aromatic ring at positions C-3, C-4 (Fig. 1). This led us to conclude that the *gem*-dimethylchromene moiety was also fused in an angular manner on the same ring, but at positions C-1, C-2. This was confirmed by HMBC correlations of H-13 with C-2 and C-9a, and of H-14 with C-1 (Fig. 1). Consequently, compound **3** was established as a new dibenzofuran derivative.

Paucinervin D (**4**), obtained as light yellow oil, gave the molecular formula $C_{27}H_{40}O_3$, as revealed by its HRESIMS at *m/z* 411.2901 $[M-H]^-$. The NMR data for **4** were similar to those of known compound, parvifoliol F,[18] with differences in substitutes at aromatic ring only. Compound **4** exhibited UV absorption bands at 208 and 295 nm while a hydroxyl stretching band (3400 cm^{-1}) was the only significant absorption observed in the IR spectrum. The ^{1}H NMR spectrum (Table 2) displayed resonances of one aromatic proton (δ_H 6.43, s), four methylene protons of chroman ring [δ_H 2.58 (2H, t, J = 6.6 Hz) and 1.74–1.80 (2H, m)], one 4,8,12-trimethyltrideca-3,7,11-trienyl unit [δ_H 5.11 (1H, t, J = 7.2 Hz), 5.06 (2H, t, J = 7.2 Hz), 1.48–1.52 (2H, m), 2.09–2.13 (2H, m), 1.92–1.97 (4H, m), 2.04–2.09 (4H, m), 1.54 (3H, s), 2.02 (3H, s), 1.64 (3H, s), and 1.56 (3H, s)], one aromatic methyl group (δ_H 2.04, 3H, s), and one oxyquaternary methyl group (δ_H 1.22, 3H, s). The presence of the 4,8,12-trimethyltrideca-3,7,11-trienyl moiety was established through COSY, HMQC, and HMBC correlations. The singlet aromatic proton at 6.43 was assigned as H-4, according to its HMBC correlations with C-2 (δ_C 124.4), C-3 (δ_C 157.4), C-5 (δ_C 146.3), and C-27 (δ_C 16.1) (Fig. 1). In the HMQC spectrum, C-5 and C-6 were correlated with H_2-7 (δ_H 2.58) of the chroman ring and H_3-27 (δ_H 2.04), respectively (Fig. 1). These results also indicated there was attachment of Me-27 at C-5 (δ_C 146.3) and fusion of the chroman ring at C-1 (δ_C 148.2) and C-6 (δ_C 121.3). The HMBC cross-peaks between the other methylene protons (δ_H 1.74–1.78, H_2-8) of the chroman ring and C-6 (δ_C 121.3), C-9 (δ_C 75.2), C-10 (δ_C 40.2), and C-11 (δ_C 24.2) confirmed there was fusion of the chroman ring at C-6 with an ether linkage at C-1 forming the linkage between the oxyquaternary methyl and 4,8,12-trimethyltrideca-3,7,11-trienyl groups at C-9 of the chroman skeleton (Fig. 1). The remaining aromatic hydroxyl groups were attached to C-2 (δ_C 124.4) and C-3 (δ_C 157.4) based on the observed chemical shifts and its molecular formula, which indicated the presence of two adjacent oxy-substituents. These data, together with other results from 2D NMR analysis confirmed the structure of compound **4**, which was named paucinervin D.

2.2. Biological activity

2.2.1. Detection of apoptosis by a caspase sensor

All 19 compounds isolated from *G. paucinervis* were evaluated for their apoptosis-inducing effects using genetically engineered HeLa-C3 cells that possess a fluorescence resonance energy transfer (FRET)-based biosensor capable of detecting caspase-3 activation.[24] These cells can emit green light under normal growth conditions and shift to blue light emission when caspase-3 is activated during apoptosis where the sensor protein inside the cells is cleaved. This color change allows direct measurement of the degree of caspase-3 activation and thus the extent of apoptosis by a fluorescent plate reader in a non-invasive way.[25]

Caspase activation was determined by measuring the fluorescent emission intensities from yellow fluorescent protein (YFP) and cyan fluorescent protein (CYP) and expressed as emission ration of YFP/CYP. In the present system, the emission ratio of YFP/CFP is usually between 6 and 8 in normal cells, and this ratio will decrease to a value of 3 or below when great majority of the cells undergo caspase-dependent apoptotic cell death. Therefore, any compound that can reduce the YFP/CFP emission ratio to a value of 3 or below is considered positive in activating apoptosis in our assay. As shown in Table 3, compounds were tested at the concentrations of 10, 25, 50, and 100 μM. Among the 19 tested compounds, excluding **13**, **18**, and **19**, the rest of them were found to reduce the YFP/CFP emission ratio below 3 within 72 h at the indicated compound concentrations. Characteristics of apoptotic cell morphology (cell shrinkage and detachment) were observed from cells treated with compounds of **2**, **9**, **14** (Fig. 2) and **5**, **6**, **8**, **10**, **11** (Supplementary Fig. 9) at 25 μM. From the kinetic profile of caspase-3 activation shown in Figure 3 and Supplementary Figure 10, at the concentration of 25 μM, compounds **8–10** reduced YFP/CFP emission ratio within 24 h (Fig. 3A), followed by compounds **2, 5**, **14** at 48 h (Fig. 3B) and compounds **6** and **11** at 72 h (Supplementary Fig. 10). The results implied that compounds **8–10** may be more effective in caspase-3 activation than the other compounds. However, further caspase assay using lower concentrations of compounds showed that compound **14** is the only compound among the 19 tested compounds that reduced the YFP/CFP emission ratio below 3 within 72 h at 10 μM indicating this compound is the most potent one to induce apoptosis (Table 3).

Compound **18** did not show any effects in inducing apoptosis in HeLa-C3 cells at 100 μM or lower concentrations. Compounds **13** and **19** were found to induce HeLa-C3 cell death before activating

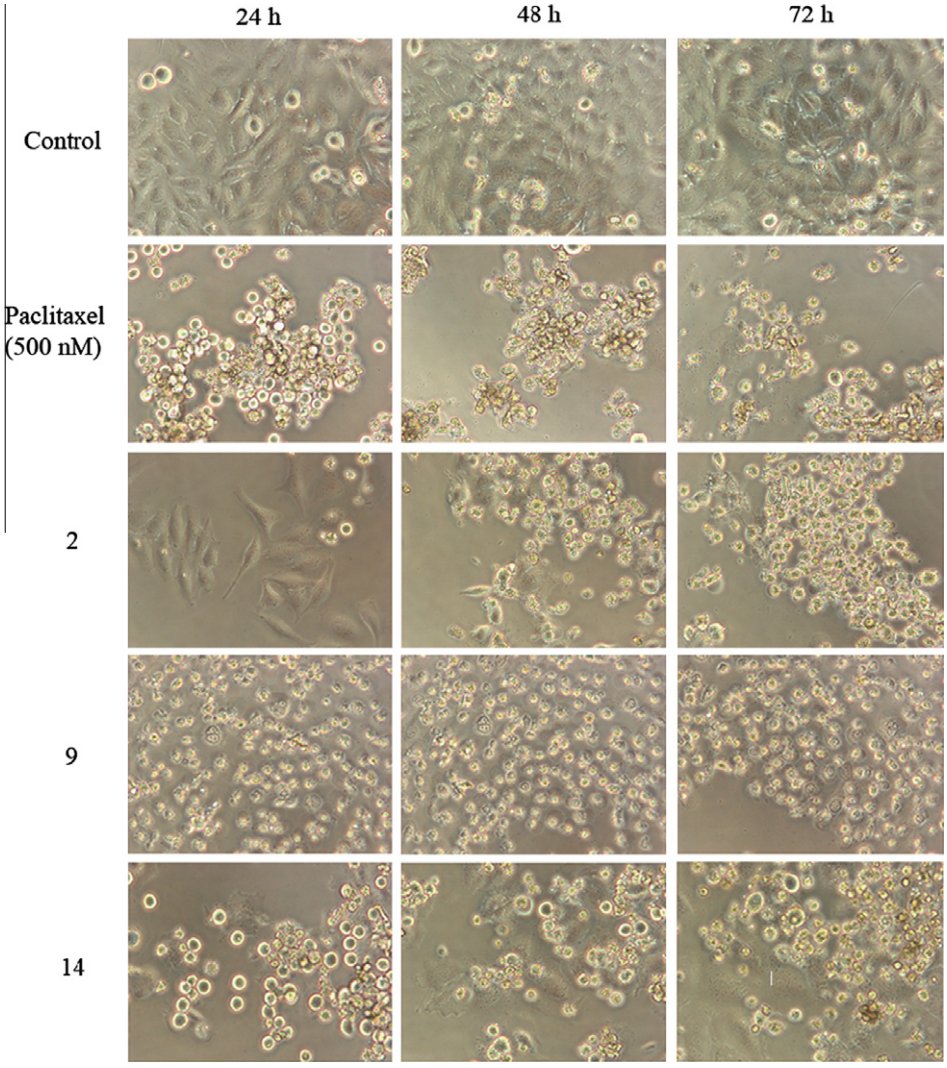

Figure 2. HeLa-C3 cell morphology during the course of treatment with compounds **2**, **9**, and **14** at 25 μM for 24, 48, and 72 h; paclitaxel at 500 nM as the positive control, culture medium containing 0.1% DMSO as the negative control.

the caspase 3 and did not reduce the YFP/CFP emission ratio to 3 within 72 h at 100 μM or lower concentrations. For **9** and **14**, at higher concentrations of 50–100 μM, they may induce HeLa-C3 cell death in apoptosis-independent pathway, resulting in no significant reduction of YFP/CFP emission ratio.

2.2.2. Cell morphological analysis for apoptosis-inducing compounds

Cell morphology analysis was used to confirm the results of in vivo apoptotic assay. HeLa-C3 cells were treated with compounds **2**, **5**, **6**, **8**, **9**–**11**, and **14** at 25 μM, for a period of three days. An anticancer drug, paclitaxel, at 500 nM was used as a positive control to treat HeLa-C3 cells. At three time points after the drug treatment (24, 48, and 72 h), cell morphology were recorded. The cells without drug treatment was used as control cells which displayed normal attached cell morphology, while cells treated with apoptotic inducer, paclitaxel, shrunk and detached from the culture plate. We also observed typical cell shrinkage and detachment from cells treated with compounds of **2**, **9**, **14** (Fig. 2) and **5**, **6**, **8**, **10**, **11** (Supplementary Fig. 9) at 25 μM. The time profiles of cell shrinkage matches well with the kinetics of caspase activation shown in Figure 3 and Supplementary Figure 10 further validated results obtained from our caspase sensor-based apoptotic assay.

2.2.3. Western blot analysis for compounds 2, 9, and 14

Western blot was used to confirm the apoptosis-inducing effects of compounds **2**, **9**, and **14**. As shown in Figure 4, after 12 h treatment of compounds **2**, **9**, and **14** at 25 μM to HeLa cells, respectively, there was little cleavage of PARP, which was a caspase-3 substrate protein for compounds **2** and **14**, but a small amount of PARP cleavage for compound **9**. However, after 36 h treatment of these compounds, there was clear cleavage of PARP into its smaller fragment from cells treated with all three compounds. Taken together, these results demonstrated that caspase-3 was activated while compounds **2**, **9**, and **14** induced HeLa cells apoptosis.

2.2.4. Evaluation of cell viability and cytotoxicity of apoptosis-inducing compounds

The rate of cell proliferation was further measured using MTT assay and the results in Figure 5 showed that compounds **2**, **5**, **6**, **8**–**11**, and **14** can significantly reduce the viability of HeLa cells at the concentration of 25 μM. In order to compare the cytotoxicity of four new compounds, we measured their IC_{50} on HeLa cells. As the results shown in Table 4, the IC_{50} of compound **2** is below 10 μM, which means that this compound has the strongest inhibition effect against HeLa cell growth than the other three newly

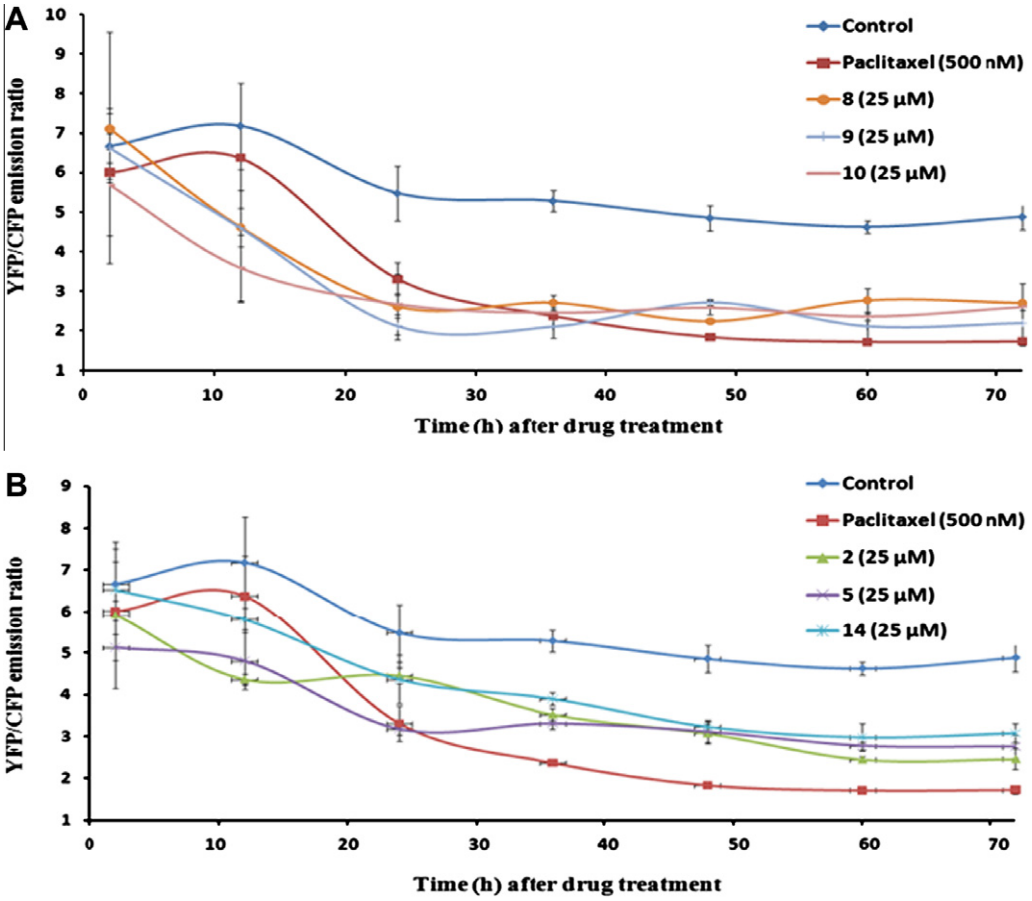

Figure 3. (A) YFP/CFP emission ratio of compounds **8**–**10** at 25 μM; paclitaxel at 500 nM as the positive control, culture medium containing 0.1% DMSO as the negative control. (B) YFP/CFP emission ratio of compounds **2**, **5**, and **14** at 25 μM; paclitaxel at 500 nM as the positive control, culture medium containing 0.1% DMSO as the negative control.

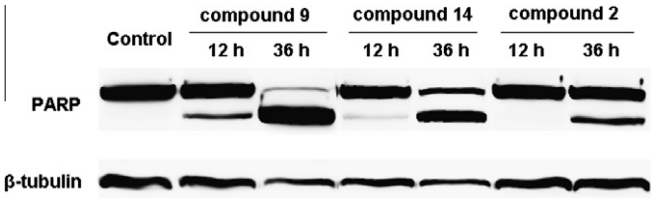

Figure 4. PARP cleavages were observed after compounds **2**, **9**, and **14** treatment. HeLa cells were treated with 25 μM of compounds **2**, **9**, and **14** for 12 and 36 h, respectively. β-Tubulin was probed as a loading control. HeLa cells treated with culture medium containing 0.1% DMSO were used as a negative control.

isolated compounds. Interestingly, although the main structures of compounds **1** and **2** are similar, compound **1** showed neither apoptosis-inducing effect nor cytotoxicity (IC_{50} = 95.6 ± 5.5 μM) against HeLa cell (Tables 3 and 4). The results demonstrated that the ester group between C-8a and C-9a may affect the apoptotic activity of this compound.

In summary, among the 19 compounds isolated from *G. paucinervis*, eight compounds reduced YFP/CFP emission ratio of HeLa-C3 cells close to or below 3 within 72 h, resulting in detached cell morphology and cell shrinkage as well as low cell viability at a low concentration of 25 μM. Compounds **8–10** and **14** demon-

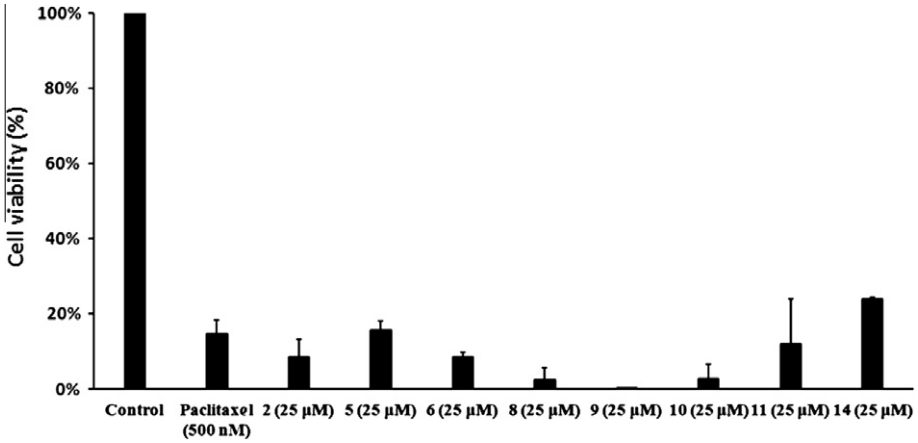

Figure 5. HeLa-C3 cell viability after 72 h treatment with compounds **2**, **5**, **6**, **8**–**11**, **14** at 25 μM. The values are expressed as means ± SD (n = 3).

Table 3
Apoptosis-inducing effects of tested compounds at 72 h

Compound	Apoptotic effect at			
	100 μM	50 μM	25 μM	10 μM
1	+	–	–	–
2	+	+	+	–
3	+	–	–	–
4	+	+	–	–
5	+	+	+	–
6	+	+	+	–
7	+	+	–	–
8	+	+	+	–
9[a]	–	–	+	–
10	+	+	+	–
11	+	+	+	–
12	+	+	–	–
13[a]	–	–	–	–
14[a]	+	–	+	+
15	+	+	–	–
16	+	–	–	–
17	+	+	–	–
18	–	–	–	–
19[a]	–	–	–	–

'+' means the YFP/CFP emission ratio of compound treated HeLa-C3 cells was 3 or below 3 at 72 h. '–' means the YFP/CFP emission ratio of compound treated HeLa-C3 cells was above 3 at 72 h. The compounds which are labeled with 'a' means that they may induce HeLa-C3 cell death in an apoptosis-independent manner at certain concentrations.

Table 4
IC_{50} values of four new compounds at 72 h on HeLa cells

Compound	IC_{50} (μM)
1	95.6 ± 5.5
2	9.5 ± 0.2
3	52.5 ± 1.5
4	29.5 ± 0.2

strated stronger apoptosis-inducing effects and they can be considered as potential anticancer drug candidates.

3. Experimental

3.1. General experimental procedures

Optical rotations were measured by a JASCO DIP-1000 polarimeter. Ultraviolet absorption spectra were recorded using a Perkin–Elmer Lambda L14 spectrometer. A Perkin–Elmer spectrum 100 FT-IR spectrometer was used for scanning IR spectroscopy with KBr pellets. The 1D and 2D NMR spectra were recorded on a Bruker AV-400 spectrometer with TMS as internal standard. Chemical shifts (δ) were expressed in ppm with reference to the solvent signals. HRMS were obtained using a nanoLC–MS/MS system, with a nanoAcquity ultra-performance liquid chromatography (UPLC) module and a quadrupole time-of-flight (Q-TOF) spectrometer equipped with a nanoelectrospray ion source (Waters, Milford, MA) and connected to a lock-mass apparatus to perform a real-time calibration correction. Column chromatography was performed with silica gel (200–300 mesh, Qingdao Marine Chemical Inc.), Sephadex LH-20 (Pharmacia), and reversed-phase C18 silica gel (250 meshes, Merck). Precoated TLC sheets of Silica Gel 60 GF_{254} were used. An Agilent 1100 series equipped with an Alltima C18 column (4.6 × 250 mm) was used for HPLC analysis, and semi-preparative and preparative Alltima C18 columns or Zorbax SB-C18 columns (9.4 × 250 mm and 22 × 250 mm) were used in sample preparation. Spots were visualized by heating silica gel plates sprayed with 10% H_2SO_4 in EtOH.

3.2. Plant material

The leaves of *G. paucinervis* were collected in October 2008 from Xishuangbanna Prefecture of Yunnan Province, China. The plant was identified by Pan-Yu Ren, a pharmacognosist. A voucher specimen (CMED-047404) has been deposited at Hong Kong Jockey Club Institute of Chinese Medicine.

3.3. Extraction and isolation

Air-dried and powdered leaves (2.8 kg) were extracted with Me_2CO (15 L) for three times at room temperature and concentrated in vacuo to give a crude extract, which was partitioned between H_2O and CH_2Cl_2. The CH_2Cl_2-soluble portion (182 g) was decolorized by MCI. The 90% methanol part (57 g) was chromatographed on a silica gel column eluting with hexane–acetone (1:0, 40:1, 9:1, 8:2, 7:3, 1:1, and 0:1) to afford five fractions, I–V.

Fraction I (6 g) was performed on reversed-phase column (RP-18) eluting with MeOH–H_2O (30–90%) to give 23 fractions. Fractions I-11 (587 mg), I-14 (234 mg), I-15 (85 mg), I-18 (43 mg) were separately subjected to semi-preparative HPLC (MeOH–H_2O, 60:40) to yield compounds **17** (75 mg), **18** (8 mg), **4** (62 mg), **16** (9 mg), **19** (7 mg), **5** (7 mg), and **6** (6 mg). Fraction II-1 (7 g) was then performed on reversed-phase column (RP-18) eluting with MeOH–H_2O (80–100%) to give 17 fractions. Fractions II-1–7, II-1–9, II-1–10 were separated over Sephadex LH-20 eluting with MeOH and then subjected to semi-preparative HPLC (MeOH–H_2O, 80:20) to yield **1** (3 mg), **2** (4 mg), **3** (10 mg), **11** (3 mg), **12** (5 mg), and **15** (4 mg). Fraction II-2 (4 mg) was separated over Sephadex LH-20 eluting with MeOH and then subjected to semi-preparative HPLC (MeOH–H_2O, 60:40) to yield compounds **7** (2 mg), **8** (6 mg), **9** (4 mg), **13** (3 mg), and **14** (2 mg).

3.3.1. Paucinervin A (1)

Yellow gum; $[\alpha]_D^{24}$ – 3.7 (*c* 0.61, MeOH); UV (MeOH) λ_{max} (log ε) 278 (2.25), 250 (1.98), 220 (2.55) nm; IR (KBr) ν_{max} 3411, 2924, 1624, 1493, 1465, 1424, 1384, 1283, 1201, 1146, 1069, 982 cm^{-1}; ^1H and ^{13}C NMR data, Table 1; positive HRESIMS *m/z* 427.1694 $[M+H]^+$ (calcd 427.1757 for $C_{24}H_{27}O_7$).

3.3.2. Paucinervin B (2)

Brown gum; $[\alpha]_D^{24}$ – 3.8 (*c* 0.26, MeOH); UV (MeOH) λ_{max} (log ε) 267 (2.36), 245 (2.04), 225 (2.71) nm; IR (KBr) ν_{max} 3411, 2928, 1621, 1438, 1370, 1320, 1265, 1193, 1114, 1069 cm^{-1}; ^1H and ^{13}C NMR data, Table 1; positive HRESIMS *m/z* 405.1540 $[M+H]^+$ (calcd 405.1549 for $C_{21}H_{25}O_8$).

3.3.3. Paucinervin C (3)

White gum; $[\alpha]_D^{24}$ – 39.5 (*c* 0.72, MeOH); UV (MeOH) λ_{max} (log ε) 280 (2.33), 267 (2.48), 247 (2.34) nm; IR (KBr) ν_{max} 3400, 2925, 1619, 1461, 1384, 1158, 1110, 1065, 1050, 1022 cm^{-1}; ^1H and ^{13}C NMR data, Table 1; negative HRESIMS *m/z* 305.0509 $[M-H]^-$ (calcd 305.0814 for $C_{19}H_{13}O_4$).

3.3.4. Paucinervin D (4)

Light yellow oil; $[\alpha]_D^{24}$ – 6.8 (*c* 1.92, MeOH); UV (MeOH) λ_{max} (log ε) 295 (1.13), 208 (2.10) nm; IR (KBr) ν_{max} 3400, 2969, 2925, 2855, 1618, 1460, 1414, 1377, 1308, 1231, 1165, 1106, 1061, 1005, 973, 928, 857 cm^{-1}; ^1H and ^{13}C NMR data, Table 2; negative HRESIMS *m/z* 411.2901 $[M-H]^-$ (calcd 411.2899 for $C_{27}H_{39}O_3$).

3.4. Bioassay

The bioassay method was described in our previous paper with some modifications.[25] All the testing samples were dissolved in DMSO to make stock solutions. The concentration of each stock

was at least 1000 times higher than the working concentration. HeLa-C3 cells, which can detect apoptotic cell death involving caspase activation, were cultured in minimum essential medium (MEM) containing 10% fetal bovine serum, 100 U/mL penicillin, 100 mg/mL streptomycin, in a 5% CO_2 humidified incubator at 37 °C. Each sample well for apoptotic activity testing was prepared by seeding 7500 HeLa-C3 cells suspended in 100 μL culture medium. After 12–16 h incubation, the old medium was removed and 100 μL freshly prepared culture medium containing the testing sample at a certain working concentration was added to the sample wells and fresh medium only to the corresponding background wells. Culture medium containing 0.1% DMSO was used as a negative control while 500 nM paclitaxel was added as the positive control. After that, the plate was read by a Perkin–Elmer Victor reader with excitation wavelength at 440 ± 10 nm and emission wavelength at 486 ± 8 nm for cyan fluorescent protein (CFP) and 535 ± 8 nm for yellow fluorescent protein (YFP) at the indicated time points. The data acquisition duration was up to 72 h. The YFP/CFP emission ratio was then calculated. Furthermore, the cell morphological images were captured at 24 h, 48 h, and 72 h after treatment with Leica DMIL HC equipped with Leica DFC300FX camera. If YFP/CFP emission ratio was reduced to or below 3 and the cell shrinkage was observed, the testing sample was considered as a positive apoptotic inducer at that concentration. All samples were tested in triplicates. The whole experiment was repeated for three times.

Western blot analysis was used to confirm the apoptosis-inducing effects of compounds **2**, **9**, and **14**. HeLa cells were treated with compounds **2**, **9**, and **14** at 25 μM, and at two time points after drug treatment (12 h, 36 h), cells were harvested and lysed. Cell lysate containing 100 μg of protein was separated by 12% SDS–PAGE and transferred onto an Amersham Hybond ECL nitrocellulose membrane (GE Healthcare, Waukesha, WI). After blocking with 5% non-fat milk, the membranes were incubated with one of the following primary antibodies at 1:1000 dilutions for overnight at 4 °C: rabbit anti-β-tubulin (Cell Signaling Technology, #2146), and mouse anti-PARP (F-2) (Santa Cruz Biotechnology, sc-8007). The membranes were then incubated with one of the following horseradish peroxidase-conjugated secondary antibodies at 1:2500 dilutions at room temperature for 1 h: goat-anti-rabbit (Bio-Rad, Carlsbad, CA, 170-6515) or goat-anti-mouse (Bio-Rad, 170-6516) and developed using Amersham ECLTM Western-blotting analysis system (GE Healthcare).

The cell viability was also determined by MTT assay. MTT powder was dissolved in PBS at a concentration of 5 mg/mL. After 72 h treatment, 10 μL of MTT solution was added into each well of a 96-well plate. After 2 h incubation at 37 °C, 100 μL 10% SDS solution with 0.01 M HCl was added to dissolve the purple crystals. After 24 h incubation, the optical density (OD) readings at 595 nm were measured using a plate reader. The viability of cells treated with compound was equal to its OD reading divided by that of control. (The value is expressed as the form of percentage.)

We measured the IC_{50} values of four new compounds using MTT assay. Firstly, 2500 HeLa cells suspended in 100 μL MEM medium were seeded, respectively, in a 96-well plate. After 24 h incubation, fresh medium containing various concentrations of each compound were added into the 96-well plate to replace the old medium. The concentrations applied except **1** which was from 200 μM to 3.125 μM were ranged from 100 μM to 1.5625 μM, which was achieved by doing twofold dilutions for six times. The OD_{595} values of the control groups at 0 h and 72 h together with the compound treated groups at 72 h from the MTT assay were measured using a plate reader. IC_{50} is the concentration of a compound inhibiting 50% of the cell growth.

Acknowledgments

This research was funded by the Hong Kong Jockey Club Charities Trust and School of Chemical and Biomedical Engineering start-up funds of Nanyang Technological University.

Supplementary data

Supplementary data associated with this article can be found, in the online version, at doi:10.1016/j.bmc.2010.06.014.

References and notes

1. Kerr, J. F.; Wyllie, A. H.; Currie, A. R. *Br. J. Cancer* **1972**, *26*, 239.
2. Samali, A.; Zhivotovsky, B.; Jones, D.; Nagata, S.; Orrenius, S. *Cell Death Differ.* **1999**, *6*, 495.
3. Huang, S. X.; Feng, C.; Zhou, Y.; Xu, G.; Han, Q. B.; Qiao, C. F.; Chang, D. C.; Luo, K. Q.; Xu, H. X. *J. Nat. Prod.* **2009**, *72*, 130.
4. Xu, G.; Feng, C.; Zhou, Y.; Han, Q. B.; Qiao, C. F.; Huang, S. X.; Chang, D. C.; Zhao, Q. S.; Luo, K. Q.; Xu, H. X. *J. Agric. Food Chem.* **2008**, *56*, 11144.
5. Han, Q. B.; Tian, H. L.; Yang, N. Y.; Qiao, C. F.; Song, J. Z.; Chang, D. C.; Luo, K. Q.; Xu, H. X. *Chem. Biodivers.* **2008**, *5*, 2710.
6. Han, Q. B.; Zhou, Y.; Feng, C.; Xu, G.; Huang, S. X.; Li, S. L.; Qiao, C. F.; Song, J. Z.; Chang, D. C.; Luo, K. Q.; Xu, H. X. *J. Chromatogr. B Analyt. Technol. Biomed. Life Sci.* **2009**, *877*, 401.
7. Yang, N. Y.; Han, Q. B.; Cao, X. W.; Qiao, C. F.; Song, J. Z.; Chen, S. L.; Yang, D. J.; Yiu, H.; Xu, H. X. *Chem. Pharm. Bull. (Tokyo)* **2007**, *55*, 950.
8. Han, Q. B.; Wang, Y. L.; Yang, L.; Tso, T. F.; Qiao, C. F.; Song, J. Z.; Xu, L. J.; Chen, S. L.; Yang, D. J.; Xu, H. X. *Chem. Pharm. Bull. (Tokyo)* **2006**, *54*, 265.
9. Han, Q. B.; Yang, N. Y.; Tian, H. L.; Qiao, C. F.; Song, J. Z.; Chang, D. C.; Chen, S. L.; Luo, K. Q.; Xu, H. X. *Phytochemistry* **2008**, *69*, 2187.
10. Li, X. W. In *Floral of China*; Li, X. W., Li, Y. H., Tong, S. Q., Tao, G. D., Zhang, P. Y., Zhang, Y. J., Eds.; Science Press: Beijing, 1998; Vol. 50, pp 101–102.
11. Roux, D.; Hadi, H. A.; Thoret, S.; Guenard, D.; Thoison, O.; Pais, M.; Sevenet, T. *J. Nat. Prod.* **2000**, *63*, 1070.
12. Herath, K.; Jayasuriya, H.; Ondeyka, J. G.; Guan, Z.; Borris, R. P.; Stijfhoorn, E.; Stevenson, D.; Wang, J.; Sharma, N.; Macnaul, K.; Menke, J. G.; Ali, A.; Schulman, M. J.; Singh, S. B. *J. Nat. Prod.* **2005**, *68*, 617.
13. Fuller, R. W.; Blunt, J. W.; Boswell, J. L.; Cardellina, J. H., II; Boyd, M. R. *J. Nat. Prod.* **1999**, *62*, 130.
14. Shen, J.; Yang, J. S. *Huaxue Xuebao* **2007**, *65*, 1675.
15. Xu, G.; Kan, W. L. T.; Zhou, Y.; Song, J. Z.; Han, Q. B.; Qiao, C. F.; Cho, C. H.; Rudd, J. A.; Lin, G.; Xu, H. X. J. *J. Nat. Prod.* **2010**, *73*, 104.
16. Lee, S. B.; Chen, C. M. U.S. Pat. Appl. Publ. 2005, 22p.
17. Rukachaisirikul, V.; Naklue, W.; Phongpaichit, S.; Towatana, N. H.; Maneenoon, K. *Tetrahedron* **2006**, *62*, 8578.
18. Ito, C.; Miyamoto, Y.; Rao, K. S.; Furukawa, H. *Chem. Pharm. Bull.* **1996**, *44*, 441.
19. Zhong, F. F.; Chen, Y.; Wang, P.; Feng, H. J.; Yang, G. Z. *Chin. J. Chem.* **2009**, *27*, 74.
20. Rukachaisirikul, V.; Ritthiwigrom, T.; Pinsa, A.; Sawangchote, P.; Taylor, W. C. *Phytochemistry* **2003**, *64*, 1149.
21. Mattern, D. L.; Scott, W. D.; McDaniel, C. A.; Weldon, P. J.; Graves, D. E. *J. Nat. Prod.* **1997**, *60*, 828.
22. Kamisaka, H.; Shaku, M. *Moisturizing Cosmetics containing Hydrogenated Retinols*; Kokai Tokkyo Koho: Japan, 1989, 5p.
23. Dowd, P.; Zheng, Z. B. *Proc. Natl. Acad. Sci. U.S.A.* **1995**, *92*, 8171.
24. Luo, K. Q.; Yu, V. C.; Pu, Y.; Chang, D. C. *Biochem. Biophys. Res. Commun.* **2001**, *283*, 1054.
25. Tian, H.; Ip, L.; Luo, H.; Chang, D. C.; Luo, K. Q. *Br. J. Pharmacol.* **2007**, *150*, 321.